Analytica Chimica Acta 726 (2012) 79–84

Contents lists available at SciVerse ScienceDirect

Analytica Chimica Acta

journal homepage: www.elsevier.com/locate/aca

Ultrasensitive detection of ovarian cancer marker using immunoliposomes and gold nanoelectrodes

Subramanian Viswanathan[a,*], Chinnakkaruppanan Rani[b], Cristina Delerue-Matos[a]

[a] REQUIMTE, Instituto Superior de Engenharia do Porto, R.S. Tomé, 4200-072 Porto, Portugal
[b] Department of Chemistry, Thiru. Vi. Ka. Government Arts College, Thiruvarur 610003, Tamilnadu, India

ARTICLE INFO

Article history:
Received 28 November 2011
Received in revised form 8 March 2012
Accepted 14 March 2012
Available online 23 March 2012

Keywords:
Immunosensor
Ovarian cancer
Mucin-16
Gold nanoelectrodes
Liposome

ABSTRACT

Mucin-16 (MUC16) is the established ovarian cancer marker used to follow the disease during or after treatment for epithelial ovarian cancer. The emerging science of cancer markers also demands for the new sensitive detection methods. In this work, we have developed an electrochemical immunosensor for antigen MUC16 using gold nanoelectrode ensemble (GNEE) and ferrocene carboxylic acid encapsulated liposomes tethered with monoclonal anti-Mucin-16 antibodies (αMUC16). GNEEs were fabricated by electroless deposition of the gold within the pores of polycarbonate track-etched membranes. Afterwards, αMUC16 were immobilized on preformed self-assembled monolayer of cysteamine on the GNEE via cross-linking with EDC-Sulfo-NHS. A sandwich immunoassay was performed on αMUC16 functionalized GNEE with MUC16 and immunoliposomes. The differential pulse voltammetry was employed to quantify the faradic redox response of ferrocene carboxylic acid released from immunoliposomes. The dose–response curve for MUC16 concentration was found between the range of 0.001–300 U mL^{-1}. The lowest detection limit was found to be 5×10^{-4} U mL^{-1} (S/N = 3). We evaluated the performance of this developed immunosensor with commercial ELISA assay by comparing results obtained from spiked serum samples and real blood serum samples from volunteers.

1. Introduction

Epithelial ovarian cancer is one of the most frequent causes of all female cancer-related deaths in the western world. Ovarian cancer is that forms in tissues of the ovary. Most ovarian cancers are either ovarian epithelial carcinomas or malignant germ cell tumors. Ovarian cancer symptoms are often vague. The majority ovarian cancers are detected at a late stage resulting in high mortality rates. Thus, it is essential to develop simple and inexpensive methods for early detection and screening of ovarian cancer [1,2]. Over a decade of omics investigations have identified many potential biomarkers for ovarian cancer. A cancer marker mucin-16 (MUC16), also named as cancer antigen-125 (CA-125) is a high-molecular-weight glycoprotein found on the surface of many ovarian cancer cells [3,4]. Early Detection Research Network, a program run by the National Cancer Institute (NCI), released its evaluation of the performance of 35 previously reported markers of ovarian cancer [5]. When the researchers evaluated the biomarkers in 180 diseases, and 660 control specimens obtained as part of NCI's Prostate, Lung, Colorectal & Ovarian Cancer Screening Trial, none of the new markers was better than MUC16, after all [6]. Normal blood levels are usually less than 35 U mL^{-1} (units per milliliter). More than 90% of women have high levels of MUC16 when the ovarian cancer is advanced. MUC16 levels are also elevated in about half of women whose cancer has not spread outside of the ovary. Monitoring changes in serum MUC16 is an important at the time of diagnosis and during the treatment to understand the therapeutic responses.

Electrochemical biosensors offer several advantages compared to alternative or existing approaches. In general, a number of high-performing protein detection protocols are under development [7], and many of the most specific and sensitive methods use micro- and nanomaterials in their sensing schemes [8,9]. Development of nanosize electrodes constitutes one of the frontiers in electrochemical science. In principle, the electroanalytical detection limits at a nanoelectrode ensemble will be much lower than that at an analogous macro sized electrode because the ratio of faradic to the capacitive current is significantly high at ensemble electrodes. The simple colloidal chemical approach has been successfully used for the development of ultramicroelectrodes and nanoelectrode ensembles [9]. The micro or nanoelectrode ensembles have been used for the electrochemical sensors. They offer numerous benefits over the conventional macroelectrodes such as enhanced mass transport, lowered influence of the solution resistance, low detection limit, and better signal-to-noise ratio (S/N). Utilization of nanomaterials for the sensitive detection of cancer markers is an interesting area in bioanalytical research. Gold

* Corresponding author. Tel.: +351 228340500; fax: +351 228321159.
E-mail address: rsviswa@gmail.com (S. Viswanathan).

0003-2670/$ – see front matter © 2012 Elsevier B.V. All rights reserved.
doi:10.1016/j.aca.2012.03.025

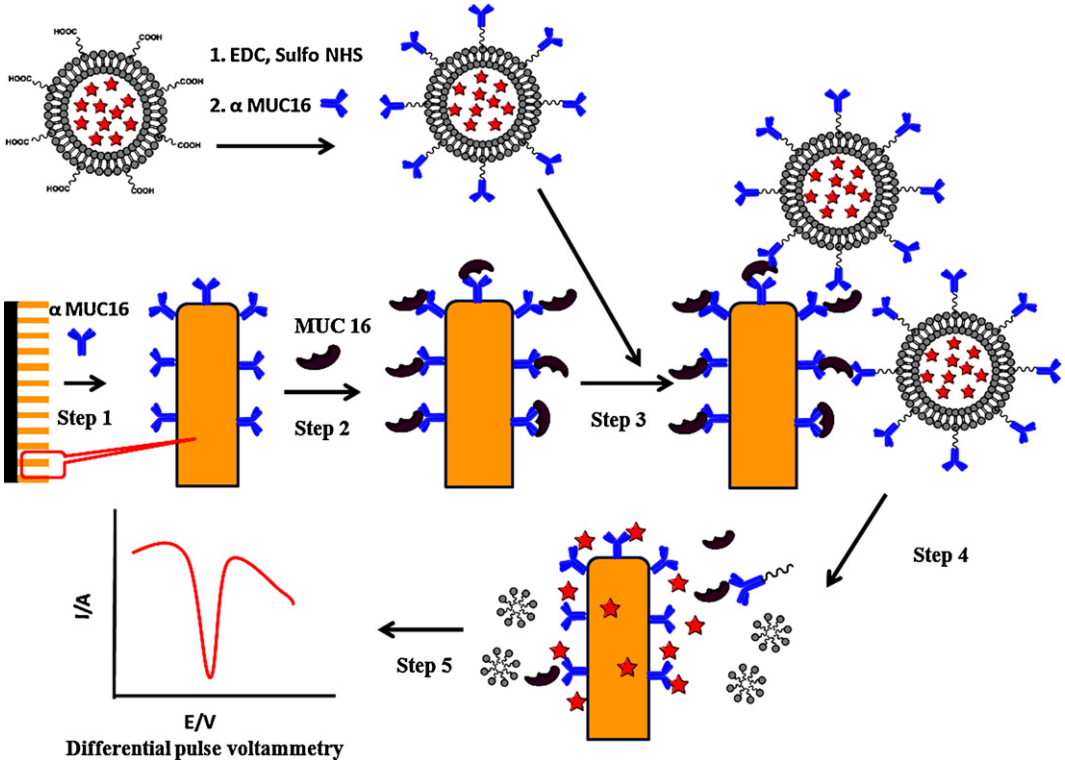

Fig. 1. Outline of liposome amplified electrochemical detection of MUC16 (antigen) using αMUC16-FcL biolables and iGNEE: step 1, αMUC16 (antibody) immobilized on electrode surface; step 2, MUC16 immunoconjugated with αMUC16 on electrode surface; step 3, sandwich immunocomplex formed with αMUC16-FcL; step 4, bound liposomes were lysed and ferrocene carboxylic acid released on the electrode surface; step 5, voltammetric response of release ferrocene carboxylic acid.

nanomaterials [10,11], carbon nanotubes [12,13], mesoporous silica [14], barcoded nanoparticles [13], enzyme-labeled beads [15,16], and micro-nanoarrays [17–19] used with electrochemical transduction revealed the eminent capability for the development of cancer marker sensors. Liposomes are spherical lipid vesicles consisting of a bilayered membrane structure that can be used as carriers of different signaling tracers with high carrying capacity and functionalized with various biomolecules for use in a variety of bioaffinity assays [20]. Application of liposomes as bio-labels to replace traditional enzyme-labels is an attractive tool in bioanalytical research. Many ultrasensitive optical and voltammetric immunoassays were also reported based on liposomes containing fluorescent dyes [21], enzymes [22] and electroactive compounds [12,23,24]. In the present investigation, considering the potential importance of the detection of MUC16 biomarker in blood serum, we have explored the sensitive determination of MUC16 level in human blood serum using αMUC16 immobilized on gold nanoelectrode ensembles and ferrocene carboxylic acid encapsulated liposomes functionalized with αMUC16 (αMUC16-FcL). As illustrated in Fig. 1, the MUC16 detection protocol involves a sandwich immunoassay, which leads to capture of the redox marker loaded liposomes, followed by a ruptured release of the electroactive signaling molecules and their electrochemical detection.

2. Experimental

2.1. Materials

Dipalmitoylphosphatidylcholine (DPPC), dipalmitoylphosphatidylglycerol (DPPG) and 1,2-distearoyl-*sn*-glycero-3-phosphoethanolamine-N-[carboxy(polyethyleneglycol)-2000] (ammonium salt) (DSPE-PEG(2000)-COOH), were purchased from Avanti Polar Lipids, Inc. (Alabaster, AL, USA). MUC16 antigen, Mouse anti-MUC16 monoclonal antibody, ELISA-MUC16 analysis kits were purchased from Abcam UK. Ferrocence carboxylic acid, human serum albumin (HSA), bovine serum albumin (BSA), solvents and all other reagents used in this study were purchased from Sigma–Aldrich. Screen-printed carbon electrode (SPE) (Ref. No. C110) were purchased from Dropsens, Spain.

2.2. Instruments

SEM images were obtained from scanning electron microscope (JEOL, Model FEI Quanta 400FEGESEM/EDAX PEGASUS X4M). All electrochemical experiments were performed using an Autolab PGSTAT 12, potentiostat/galvanostat (Autolab, Eco Chemie, Netherlands) with a three-electrode electrochemical system. Differential pulse voltammetry (DPV) was conducted using initial and final potentials versus the Ag/AgCl reference electrode are −0.3 and 0.5 V, respectively. The modulation amplitude was 50 mV, and the modulation time 0.05 s; the step potential was 2 mV and the interval time 0.1 s. An electrophoretic light scattering analyser (Coulter DELSA 440, UK) was used for characterization of the liposome size and the apparent zetapotential, ξ.

2.3. Methods

2.3.1. Preparation of the ferrocene liposome biolables

Liposomes were prepared by the reported reversed-phase evaporation method [12,24]. The lipid composition consisted of a 3:1:0.6:0.01 molar ratio of DPPC, cholesterol, DPPG, and DSPE-PEG(2000)-COOH. The electroactive redox marker, 0.2 mol L^{-1} of ferrocene carboxylic acid dissolved in 0.01 mol L^{-1} phosphate buffer saline (PBS, pH 7.0), was entrapped into the liposomes and subsequently, the liposomes were extruded using a mini extruder (Avanti Polar Lipids, AL, USA) through polycarbonate filters (1.0, 0.4 and 0.2 μm, 20 times each) at 60 °C for homogeneous solution of unilamellar vesicles. It was then purified from

the unentrapped electroactive redox marker by gel filtration using Sephadex G50 column. The liposome fraction was dialyzed for 12 h at 4 °C using 12–15 kDa molecular weight cutoff (MWCO) membrane against 0.01 mol L^{-1} PBS (pH 7.0) containing 0.02 mol L^{-1} NaCl, 0.02 mol L^{-1} sucrose and 0.01% NaN_3. The osmolarity of dialysis buffer was maintained at range 0.05–0.10 mol L^{-1} kg^{-1} by adding NaCl and sucrose.

2.3.2. Preparation of immunoliposomes

Immunoliposomes were prepared by coupling antibodies at the carboxylic group of distal terminals of DSPE-PEG(2000)-COOH. The coupling procedure involved a two-step carbodiimide reaction. Briefly, 10 mmol L^{-1} N-(3-dimethylaminopropyl)-N′-ethylcarbodiimide (EDC) and 5 mmol L^{-1} N-(3-dimethylaminopropyl)-N′-ethylcarbodiimide (Sulfo-NHS) were mixed with liposomes in the buffer solution of 0.1 mol L^{-1} 2-(N-morpholino)ethanesulfonic acid containing 0.150 mol L^{-1} NaCl (MES, pH 6.0), and the mixture was incubated for 20 min with gentle shaking at 25 °C. 2-Mercaptoethnol was added to the mixture at the final concentration of 20 mM, followed by immediate application on to a saphadex G-50 column, equilibrated with MES buffer and the liposomes fractions collected. Next, antibody was added to liposomes solutions and incubated for overnight at 4 °C. The reaction was stopped by addition of 0.01 M ethanolamine in 0.01 mol L^{-1} tris(hydroxymethyl)aminomethane hydrochloride buffered saline (TBS) (pH 7.8) and kept for 15 min at room temperature. Uncoupled αMUC16 molecules were removed from the liposomes by passing the coupling mixture through a Sapharose CL-4B column in 4-(2-hydroxyethyl)-1-piperazineethanesulfonic acid (HEPES) buffer. The liposomes were dialyzed against 0.01 mol L^{-1} TBS containing 0.02 mol L^{-1} NaCl, 0.02 mol L^{-1} sucrose and 0.01% NaN_3 (pH 7.0, osmolarity 0.05–0.10 mol L^{-1} kg^{-1}) for 12 h at 4 °C. The purified liposomes were stored in the dark at 4 °C.

2.3.3. Preparation of the gold nanoelectrode ensembles

Gold nanoelectrode ensembles were prepared by electroless deposition of the gold within the 100 nm pores of polycarbonate particle track-etched membranes. Controlled solvent etching procedure based on the solubility of polycarbonate membranes in solvent mixtures was utilized for the fabrication of the GNEE [25]. Please refer the supporting information for detailed experimental procedure.

2.3.4. Fabrication of the immunosensors

GNEE membrane was glued on the working electrode of SPE by conductive graphite ink (Acheson Electrodag PF-407 A). The antibody molecules were immobilized through the carboxylic acid groups on the GNEE surface. The mixed monolayer on GNEE was obtained by chemisorption of 2-mercaptopropionic acid (0.0005 mol L^{-1}) and 2-mercaptoethanol (0.001 mol L^{-1}) for 18 h. GNEE was treated with 5 mM sulfo-NHS and 10 mM EDC in MES buffer (pH 6.0) for 1 h to activate the carboxyl groups on the surface and rinsed with ethanol. An aliquot (20 μL) of MUC16 antibody (20 μg mL^{-1} in PBS), was then placed on the surface of the SAM modified gold nanoelectrodes and the sensor was stored at 4 °C for 24 h. The nonspecific binding of the immunosensor was blocked by 0.2 M ethanolamine and 0.1% BSA solution. This MUC16 antibody-immobilized gold nanoelectrode ensemble (iGNEE) was rinsed with a pH 7.4 PBS and stored at 4 °C prior to usage. At identical conditions, few more electrodes were prepared without antibody molecules for control experiments.

2.3.5. Assay procedure

The iGNEE were incubated for 30 min at 25 ± 3 °C with 50 μL of the MUC16 standard or spiked or real sample followed by washing with PBS (0.1 mol L^{-1}, pH 7.0). Next, iGNEE was incubated at 25 ± 3 °C for 30 min with 50 μL of optimum concentration of αMUC16-FcL and washed with PBS (0.1 mol L^{-1}, pH 7.0). Dissolution of the bound liposomes was done by the addition of 100 μL methanolic solution of Triton X (2%) in PBS (0.1 mol L^{-1}, pH 7.0). The DPV was recorded from −0.3 V to 0.5 V.

2.3.6. Serum collection

Blood serum samples were prepared by collecting venous blood samples from female volunteers in BD Vacutainer® SST™ GEL Tubes (Becton Dickinson, India). The SST tubes were allowed to clot, and the tubes were centrifuged at 1300 × *g*. The separated serum was decanted for use. The same procedures were followed for serum samples collected from healthy individuals.

2.3.7. Safety notes

Clinical serum samples are bio-hazardous and hence should be handled with great care. Carcinogenic organic solvents and harmful chemicals were used in this study and all necessary safety precautions must be taken while working with these chemicals.

3. Results and discussions

3.1. Liposome characteristics

DPPC, cholesterol, DPPG, and DSPE-PEG(2000)-COOH mixed in the molar ratio of 3:1:0.6:0.01 was used to prepare liposome. In aqueous media, PEGylated chain with carboxyl terminal was believed to extend away from the liposome into the bulk solvent as it was not attracted by the lipid bilayer [26]. Immunoliposomes were prepared by activating the free carboxyl group of the linker lipid in liposomes with EDC and sulfo-NHS. The amine-reactive sulfo-NHS ester intermediate had sufficient stability to permit two-step cross linking protocol (Fig. 1). The PEG chain extends the immunoreactivity of antibody molecules on the liposomes. The stability of liposome was also improved by the use of PEG-lipid derivatives. The size homogeneity of αMUC16-FcLs is very important in diagnostic applications to obtain reproducibility and it was found that extrusion of the liposome preparations through polycarbonate filters reduces the size heterogeneity. Three different batch samples of liposomes were analyzed to give an average value and standard deviation for the particle diameter and zeta potential. An average hydrodynamic diameter of liposomes, *d* was found to be 180 ± 10 nm. The zeta potentials were found to be −29.53 ± 4.81 mV and −35.26 ± 5.09 mV for immunoliposome and liposome, respectively. Zeta potential of liposome before antibody coupling was slightly more negative due to the presence of terminal carboxylic groups in the lipids.

The number of lipids per liposome (N_{tot}) was calculated using the following relation:

$$N_{tot} = \left(\frac{\pi}{a_L}\right)[d^2 + (d - 2t)^2] \quad (1)$$

where a_L is the average head group surface area per lipid, *d* is the hydrodynamic diameter (180 ± 10 nm) from light scattering measurements, and *t* is the bilayer thickness [27]. The molar ratio of the DSPE-PEG(2000)-COOH was very less compared with other lipids. Hence, the major constituents in this lipid composition were considered for theoretical calculation for a_L. The bilayer thickness was assumed to be 40 Å and a_L was calculated using values of 71, 45, and 19 $Å^2$ for DPPC, DPPG and cholesterol, respectively. Using these values and weighting by the mole fraction of each component, the a_L obtained for these liposomes was 40 $Å^2$/lipid. Thus N_{tot} of 1.6×10^4 lipids/liposome was calculated by Eq. (1). The numbers of αMUC16 on each liposome surface was calculated as ∼17 molecules given that 0.0022 molar fraction of DSPE-PEG(2000)-COOH successfully coupled with αMUC16. The entrapped volume

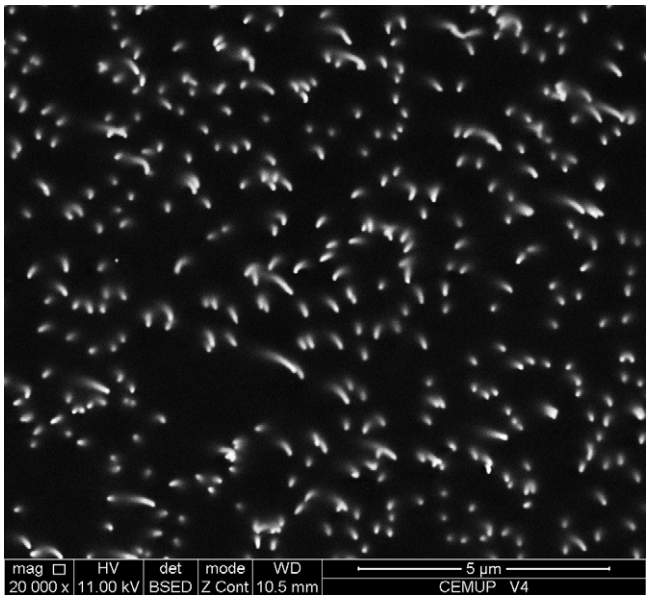

Fig. 2. Scanning electron microscopy image of a GNEE.

of the liposome (2.7×10^{-18} L) was calculated from the inner diameter. The concentration of ferrocene carboxylic acid in the liposomes cavity was 0.2 mol L^{-1}, and comparing the DPV peak current of lysed liposomes, there were $\sim 1 \times 10^{13}$ liposomes mL^{-1} and each liposome was found to contain $\sim 3.2 \times 10^{6}$ molecules of ferrocene carboxylic acid. A 10 μL aliquot of liposomes was ruptured and the amount of ferrocene carboxylic acid molecules released was measured to prove the uniformity in both liposome size and encapsulated redox marker concentration. The relative standard deviation (RSD) of these experiments was determined to be 6.4% for set of 5 replicates. RSD value indicates that the variance of ferrocarboxylic acid molecules in each liposome was very less, and practically negligible. These results confirm that the size population of the liposomes was uniformly distributed in bulk. Ferrocene carboxylic acid containing liposomes stored at 4 °C in 0.1 mol L^{-1} TBS (pH 7.0) was stable for 6 months.

3.2. Characterization of electrode

Scanning electron microscopy (SEM) surface image of the membrane shows gold nanowires with an average diameter of ~100 nm and a length of ~400 nm was shown in Fig. 2.

The SEM images clearly show GNEEs as protruding gold wires without free voids on the membrane surface. Based on this image the nanowires density was found to be ~6 nanoelectrodes μm^{-2}, which is in accordance with the declared pore density, thus confirming that each template pore was filled with gold. The results of energy dispersive X-ray measurements evidenced that this method minimized chemical contamination from the gold deposition process during the preparation of the GNEEs (Supporting information figure S1). This method provides an alternative approach to fabricate nanostructured electrode to those investigators without access to sophisticated microfabrication facilities.

The surface structure of the electrode is an important factor affecting the performance of the electrochemical immunosensor. In this work αMUC16s were immobilized on the surface of the three dimensional cylindrical GNEE electrodes. The high surface area of GNEE accommodated more numbers of αMUC16s on the electrode and it was observed that this immunoelectrode retained its immunoaffinity in all steps. Different concentrations of αMUC16s were used to immobilize αMUC16 on the GNEE to find the optimum amount of αMUC16. The efficiency of antibody immobilization was studied by the percentage of current reduction on the electrode. The percentage of current reduction was calculated by the following equation:

$$\%\ \text{of current reduction} = \left[1 - \left(\frac{I}{I_o}\right)\right] \times 100 \quad (2)$$

where I_o is the DPV peak current before antibody immobilization; I is the DPV peak current after antibody immobilization at 1 mmol L^{-1} ferrocence carboxylic acid in 0.1 mol L^{-1} PBS pH 7.4.

It was shown in Fig. 3a that the percentage of DPV peak current reduction is increased significantly when the concentration of antibody loaded on the electrode surface was changed from 0.1 to 12.0 μg mL^{-1}. With further increase in the antibody concentration to 12.0–16.0 μg mL^{-1}, there was no significant variation in the sensor response. Hence 12 μg mL^{-1} of αMUC16 was taken as the optimum concentration for immunosensor fabrication. The immunoelectrode fabrication step was crucial part in this study. At this stage, both electrochemical and immunochemical behavior of iGNEE was tested. Fig. 3b shows the DPV responses of bare GNEE, iGNEE and iGNEE incubated with 400 U mL^{-1} of MUC16 antigen at 1 mmol L^{-1} ferrocene carboxylic acid containing 0.1 mol L^{-1} PBS. These results are evident of the observation that the immunoelectrode had good selectivity towards MUC16. To select optimum incubation with antigen, iGNEE was allowed incubating with 50 μL solution of MUC16 for different periods of time. The results showed that the DPV signal increased rapidly with the incubation time up to 20 min, after which the electrode did not show any significant increase in signal and hence 20 min was selected as the optimum incubation time with antigen (Fig. 4a).

This immunoassay involved with the binding event between immunoliposomes and immunoelectrode with respect to concentration of MUC16. Amount of MUC16 bound on the electrode was amplified by αMUC16-FcL through sandwich immunocomplex formation. DPV technique was chosen for detecting the released electroactive marker from bound liposomes. The immunoliposome concentration was very important to get effective signal amplification. So, various concentration of immunoliposome was analyzed and the optimum amount was found to be 1×10^{10} liposomes mL^{-1} (Fig. 4b). The selectivity of biosensor was analyzed using 3 mg mL^{-1} human serum albumin (HSA) and HSA spiked with 0.5 U mL^{-1} MUC16 (Fig. S2). In contrast, negligible responses were observed for the corresponding control experiment without MUC16, which reflects the absence of nonspecific adsorption on immunosensor. The results were clearly indicative of the fact that the biosensor had selectivity for MUC16 detection.

3.3. Analytical calibration

The analytical calibration for MUC16 was conducted to determine the sensitivity of the immunosensor at different concentrations of MUC16 in 0.1 M PBS pH 7.0. The amount of bound αMUC16-FcL on the electrode surface is proportional to MUC16 concentration and this can be noticed from inset of Fig. 5a which displays the typical DPV responses for solutions containing different concentrations of MUC16. The calibration curve for the voltammetric detection of MUC16 was carried out by recording, for each concentration, the response of a modified electrode at optimum experimental conditions (Fig. 5). Each point of the calibration graph corresponds to the mean value obtained from five independent measurements. The current variation was observed over the range 0.001–300 U mL^{-1} with LOD 5×10^{-4} U mL^{-1}. The data were fit using *Hill* equation:

$$I(A) = 7.0 \pm 0.3 \times 10^{-6} \left[\frac{x^a}{(a^a + x^a)}\right] \quad (3)$$

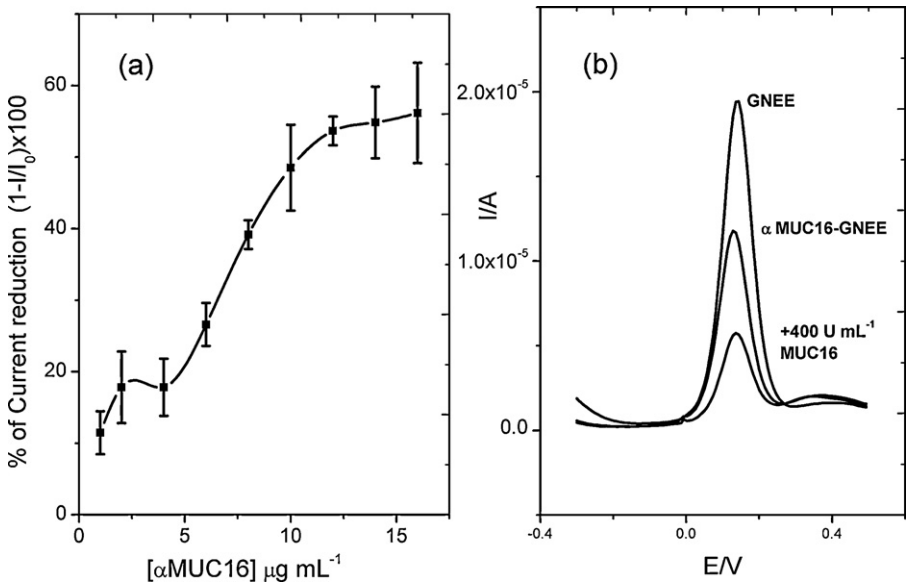

Fig. 3. (a) Effect of concentration of αMUC16 on immobilization on GNEE. I_o is the DPV peak current before antibody immobilization; I is the DPV peak current after antibody immobilization at 1 mmol L^{-1} ferrocence carboxylic acid in 0.1 mol L^{-1} PBS pH 7.4. (b) DP voltammetric responses of bare GNEE, iGNEE and iGNEE incubated with MUC16 400 U mL^{-1} at 1 mM ferrocence carboxylic acid in 0.1 mol L^{-1} PBS pH 7.4 using the DPV parameters: modulation amplitude 50 mV, and the modulation time 0.05 s; the step potential was 2 mV and the interval time 0.1 s.

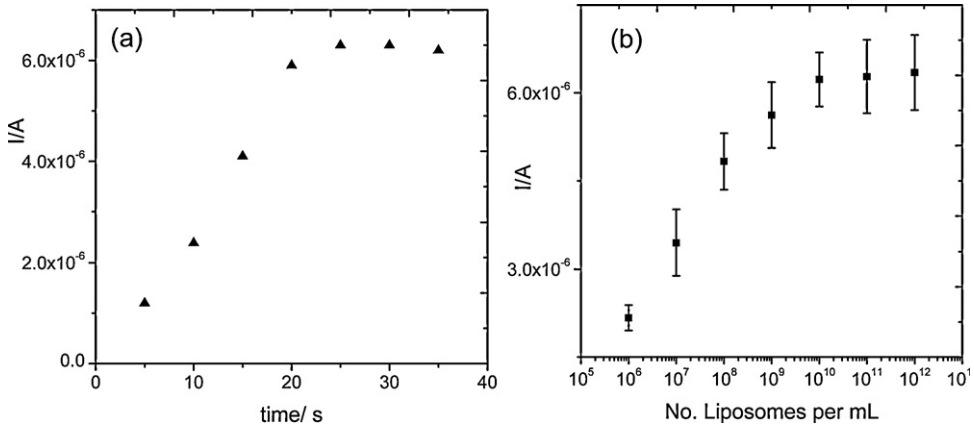

Fig. 4. (a) Effect of incubation time for immunoreactions on iGNEE with MUC 10 U mL^{-1}. (b) Influence of liposome concentrations on sensor responses at MUC 10 U mL^{-1}.

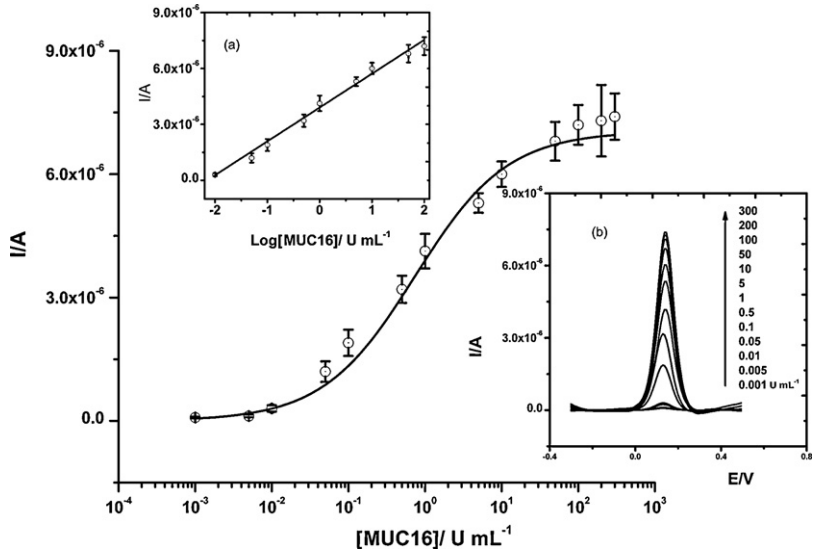

Fig. 5. MUC16 concentration-dependent peak current responses versus concentration (U mL^{-1}) on semi log plot. Inset (a), linear response of DPV current responses to MUC16. Inset (b), DP voltammograms of different MUC16 concentrations.

Table 1
Determination of MUC16 present in spiked and real human serum samples.

Source	Proposed sensor			Reference method ELISA	
	Added U mL^{-1}	Found U mL^{-1}	%RSD $n=5$	Found U mL^{-1}	%RSD $n=5$
Spiked blood serum samples	20.0	21.1	5.1	19.2	6.3
	50.0	47.8	5.8	45.4	6.1
	100.0	97.3	6.2	98.9	5.4

Source	Proposed sensor		Reference method ELISA	
	Found U mL^{-1}	%RSD $n=5$	Found U mL^{-1}	%RSD $n=5$
Infected patient[a]	75	7.9	68	8.3
Healthy person[a]	12	4.4	15	5.6

[a] Based on patient medical case history.

where $a = 0.7 \pm 0.1$, x is MUC16 concentration in U mL^{-1}.

The inset of Fig. 5a shows linear variation of Log[MUC16] with DPV current responses between the 0.01 and 100 U mL^{-1} of MUC16.

$$I(A) = (3.9 \pm 0.1 \times 10^{6}) + [(1.8 \pm 0.1 \times 10^{-6}) \times \mathrm{Log[MUC16](U\ mL^{-1})}], r^2 = 0.995 \quad (4)$$

The limit of detection (LOD) defined as the lowest concentration of MUC16 response was three times higher than the standard deviation of current response in the absence of MUC16 under identical conditions and it was found to be 5×10^{-4} U mL^{-1}. The coefficient of variation for MUC16 analysis was calculated for a set of ten independent replicates and was found to be 6.4% for 1 U mL^{-1} of MUC16. This observation indicates the reproducible nature of the immunosensor.

3.4. MUC16 in human serum samples

Quantification of serum MUC16 is an important in the ovarian cancer screening and monitoring. The developed immunosensor was then applied to the detection of MUC16 in spiked human serum samples and real samples using serum samples from cancer patient. As can be seen from Table 1, the results of the ELISA and immunosensor indicated an excellent correlation between the MUC16 levels obtained by both methods.

4. Conclusions

As a summary, we have developed the gold nanoelectrodes and liposome labels based immunosensor for the ovarian cancer marker, MUC16 detection in blood serum. The performance and clinical utility of nanoelectrodes with liposomal amplification for MUC16 were analyzed. Serum analysis using proposed biosensor is simple, making it an alternative to conventional ELISA testing, and the possibility of developing home testing kits would further facilitate it as a diagnostic aid, enabling patients to monitor their own health at home and is important for those who live far from their treatment centers. Summarily, the proposed method has potential to be further developed for practical clinic cancer biomarker diagnosis.

Acknowledgements

We thank Dr. R. Vengatesan (Dental surgeon) for his valuable help for serum sample collection. We also thank the volunteers who participated in this study.

Appendix A. Supplementary data

Supplementary data associated with this article can be found, in the online version, at doi:10.1016/j.aca.2012.03.025.

References

[1] S.M.E. Geurts, F. de Vegt, A.M. van Altena, J.A.A.M. van Dijck, V.C.G. Tjan-Heijnen, A.L.M. Verbeek, L.F.A.G. Massuger, Int. J. Gynecol. Cancer 21 (2011) 837–845.
[2] C.S. Zhu, P.F. Pinsky, D.W. Cramer, D.F. Ransohoff, P. Hartge, R.M. Pfeiffer, N. Urban, G. Mor, R.C. Bast Jr., L.E. Moore, A.E. Lokshin, M.W. McIntosh, S.J. Skates, A. Vitonis, Z. Zhang, D.C. Ward, J.T. Symanowski, A. Lomakin, E.T. Fung, P.M. Sluss, N. Scholler, K.H. Lu, A.M. Marrangoni, C. Patriotis, S. Srivastava, S.S. Buys, C.D. Berg, P.P. Team, Cancer Prev. Res. 4 (2011) 375–383.
[3] N.-J. Peng, W.-S. Liou, R.-S. Liu, C. Hu, D.-G. Tsay, C.-B. Liu, Cancer Biother. Radiopharm. 26 (2011) 175–181.
[4] M. Comamala, M. Pinard, C. Theriault, I. Matte, A. Albert, M. Boivin, J. Beaudin, A. Piche, C. Rancourt, Br. J. Cancer 104 (2011) 989–999.
[5] D.W. Cramer, R.C. Bast Jr., C.D. Berg, E.P. Diamandis, A.K. Godwin, P. Hartge, A.E. Lokshin, K.H. Lu, M.W. McIntosh, G. Mor, C. Patriotis, P.F. Pinsky, M.D. Thornquist, N. Scholler, S.J. Skates, P.M. Sluss, S. Srivastava, D.C. Ward, Z. Zhang, C.S. Zhu, N. Urban, Cancer Prev. Res. 4 (2011) 365–374.
[6] C.H. Arnaud, Chem. Eng. News 89 (2011) 40–43.
[7] J. Wang, S.-T. Yau, Biosens. Bioelectron. 29 (2011) 210–214.
[8] M. Perfezou, A. Turner, A. Merkoci, Chem. Soc. Rev. (2012), doi:10.1039/C1CS15134G.
[9] B. Kumar Jena, C. Retna Raj, Anal. Chem. 80 (2008) 4836–4844.
[10] J.-a.A. Ho, H.-C. Chang, N.-Y. Shih, L.-C. Wu, Y.-F. Chang, C.-C. Chen, C. Chou, Anal. Chem. 82 (2010) 5944–5950.
[11] Q. Wei, Y. Zhao, C. Xu, D. Wu, Y. Cai, J. He, H. Li, B. Du, M. Yang, Biosens. Bioelectron. 26 (2011) 3714–3718.
[12] S. Viswanathan, C. Rani, A.V. Anand, J.-a.A. Ho, Biosens. Bioelectron. 24 (2009) 1984–1989.
[13] X. Yu, B. Munge, V. Patel, G. Jensen, A. Bhirde, J.D. Gong, S.N. Kim, J. Gillespie, J.S. Gutkind, F. Papadimitrakopoulos, J.F. Rusling, J. Am. Chem. Soc. 128 (2006) 11199–11205.
[14] J. Lin, Z. Wei, C. Mao, Biosens. Bioelectron. 29 (2011) 40–45.
[15] D.M. Rissin, C.W. Kan, T.G. Campbell, S.C. Howes, D.R. Fournier, L. Song, T. Piech, P.P. Patel, L. Chang, A.J. Rivnak, E.P. Ferrell, J.D. Randall, G.K. Provuncher, D.R. Walt, D.C. Duffy, Nat. Biotechnol. 28 (2010) 595–599.
[16] V. Mani, B.V. Chikkaveeraiah, V. Patel, J.S. Gutkind, J.F. Rusling, ACS Nano 3 (2009) 585–594.
[17] J. Das, S.O. Kelley, Anal. Chem. 83 (2011) 1167–1172.
[18] B.V. Chikkaveeraiah, V. Mani, V. Patel, J.S. Gutkind, J.F. Rusling, Biosens. Bioelectron. 26 (2011) 44774483.
[19] H. Chen, C. Jiang, C. Yu, S. Zhang, B. Liu, J. Kong, Biosens. Bioelectron. 24 (2009) 3399–3411.
[20] K.Y. Chumbimuni-Torres, J. Wu, C. Clawson, M. Galik, A. Walter, G.-U. Flechsig, E. Bakker, L. Zhang, J. Wang, Analyst 135 (2010) 1618–1623.
[21] M. Bally, S. Syed, A. Binkert, E. Kauffmann, M. Ehrat, J. Voeroes, Anal. Biochem. 416 (2011) 145–151.
[22] B. Qu, L. Guo, X. Chu, D.-H. Wu, G.-L. Shen, R.-Q. Yu, Anal. Chim. Acta 663 (2010) 147–152.
[23] Z. Zhong, N. Peng, Y. Qing, J. Shan, M. Li, W. Guan, N. Dai, X. Gu, D. Wang, Electrochim. Acta 56 (2011) 5624–5629.
[24] S. Viswanathan, L.C. Wu, M.R. Huang, J.A.A. Ho, Anal. Chem. 78 (2006) 1115–1121.
[25] K. Krishnamoorthy, C.G. Zoski, Anal. Chem. 77 (2005) 5068–5071.
[26] C. Allen, N. Dos Santos, R. Gallagher, G.N.C. Chiu, Y. Shu, W.M. Li, S.A. Johnstone, A.S. Janoff, L.D. Mayer, M.S. Webb, M.B. Bally, Biosci. Rep. 22 (2002) 225–250.
[27] A.K. Singh, P.K. Kilpatrick, R.G. Carbonell, Biotechnol. Progr. 12 (1996) 272–280.